American Mineralogist, Volume 92, pages 80–90, 2007

The crystal chemistry of welshite, a non-centrosymmetric (*P*1) aenigmatite-sapphirine-surinamite group mineral

Edward S. Grew,[1,*] Jacques Barbier,[2] Jim Britten,[2] Ulf Hålenius,[3] and Charles K. Shearer[4]

[1]Department of Earth Sciences, University of Maine, 5790 Bryand Center, Orono, Maine 04469, U.S.A.
[2]Department of Chemistry, McMaster University, Hamilton, Ontario L8S 4M1, Canada
[3]Department of Mineralogy, Swedish Museum of Natural History, Box 50007, SE-104 05 Stockholm, Sweden
[4]Institute of Meteoritics, University of New Mexico, Albuquerque, New Mexico 87131, U.S.A.

Abstract

Previous attempts to refine the crystal structure of welshite, known only from Långban, Sweden, have been foiled by its extensive polysynthetic twinning, and without a structure determination, derivation of a reasonable formula has been difficult due its eclectic chemical composition. We report a successful refinement [w$R(F^2)$ = 0.0566 for 8048 unique reflections] in the non-centrosymmetric space group *P*1 of a relatively little twinned crystal (4% chiral) from sample NRM040068: *a* = 10.394(3) Å, *b* = 10.777(3) Å, *c* = 8.896(2) Å, α = 105.953(4)°, β = 96.294(4)°, γ = 124.948(3)°, *V* = 738.8(3) Å^3, *Z* = 1. The refined formula, $Ca_{3.78}Mg_{7.87}Sb_{3.00}Mn_{1.35}Si_{5.73}Be_{3.33}Al_{1.71}Fe^{3+}_{0.96}As_{0.27}O_{40}$, is in reasonable agreement with a formula determined by electron microprobe and Mössbauer spectroscopy (Be from the refinement), $Ca_{3.81}Mg_{7.84}Sb_{3.03}Mn_{1.17}Zn_{0.04}Fe^{2+}_{0.05}Si_{5.57}Be_{3.24}Al_{1.54}Fe^{3+}_{1.25}As_{0.37}O_{40}$. The *P*1 symmetry of welshite 040068 is mainly a result of its cation distribution, which is driven by charge ordering on both the octahedral and tetrahedral sites as supported by calculation of electrostatic site potentials. Welshite can accommodate up to 3.46 Be per 40 O atoms by including several T sites with 100% Be occupancies without the formation of unfavorable tetrahedral Be-O-Be linkages that would result in the related centrosymmetric structures of sapphirine, khmaralite, makarochkinite, and høgtuvaite, none of which contain >2.1 Be per 40 O. A generalized formula for welshite is $(Ca,Mn)_4(Mg,Mn,Fe^{2+},Fe^{3+})_9(Sb,Fe^{3+})_3O_4[(Si,As)_6(Be,Al)_4(Al,Fe^{3+})_2O_{36}]$. Compositions of most of the samples, including NRM040068, can be expressed in terms of two idealized Al and Fe end-members $Ca_4Mg_9Sb_3O_4[Si_6Be_3Al_3O_{36}]$ and $Ca_4Mg_9Sb_3O_4[Si_6Be_3AlFe_2O_{36}]$, respectively; the latter is the most representative for welshite and could be used in databases. One sample is far more heterogeneous and is irregularly zoned on scales from <1 to 10 μm. Compositional variation in this sample and in a crystal from another lie between the end-members $Ca_4Mg_{8.55}Fe_{0.45}Sb_{3.0}O_4[Si_{5.15}As_{0.45}Be_{3.45}Al_{0.5}Fe_{2.45}O_{36}]$ and $Ca_4Mg_{7.05}Fe_{3.45}Sb_{1.5}O_4[Si_{6.65}As_{0.45}Be_{3.45}Al_{0.5}Fe_{0.95}O_{36}]$, which are related by the coupled substitution $^{M}Sb^{5+} + {}^{VI}Mg^{2+} + {}^{IV}Fe^{3+} = {}^{M}Fe^{3+} + {}^{VI}Fe^{3+} + {}^{IV}Si^{4+}$, where M refers specifically to the M7, M3A, and M4A octahedral sites. The lowest measured Sb is 1.454/40 O, which may be close to the limit imposed by the need to maintain local charge balance.

Keywords: Welshite, beryllium, antimony, crystal structure, charge ordering, Mössbauer spectroscopy, electron microprobe, ion microprobe

Introduction

Welshite is one of six minerals in the aenigmatite-sapphirine-surinamite group (Strunz and Nickel 2001) to contain significant amounts of Be. We have chosen the more inclusive grouping of Strunz and Nickel (2001) because it emphasizes the close relationship of the Be-bearing minerals surinamite and sapphirine-khmaralite to makarochkinite and høgtuvaite, which are two Be minerals included in the more narrowly defined aenigmatite or aenigmatite-rhönite group (e.g., Kunzmann 1999). Welshite is also the most eclectic mineral of the aenigmatite-sapphirine-surinamite group; it invariably contains significant Mn, Fe^{3+}, and As, as well as Mg, Sb, Be, Al, and Si, constituents considered minimally essential to its formation (Hawthorne and Huminicki 2002). Moore (1967, 1971, 1978) originally introduced this mineral with the formula $Ca_4Mg_8Fe^{3+}_2Sb^{5+}_2O_4[Si_8Be_4O_{36}]$, whereas Grew et al. (2001) deduced $Ca_4Mg_{7.6}Mn^{2+}_{1.2}Fe^{2+}_{0.2}Sb^{5+}_3O_4[Si_{5.6}Be_{3.4}Fe^{3+}_{1.3}Al_{1.4}As_{0.34}O_{36}]$ from a more detailed study of its chemistry using secondary ion-microprobe spectroscopy (SIMS) to measure Be. The ion-microprobe data gave 70% more Be than the amount predicted from crystallographic studies of other Be minerals of this group, makarochkinite, høgtuvaite, khmaralite, and surinamite, in which the amount of Be did not exceed 2.1 per formula unit of 40 O or, in surinamite, 2 per 36 O (Moore and Araki 1983; Barbier et al. 1999, 2002; Grew et al. 2005). These studies showed that 95–100% of the Be is found only at the most highly polymerized tetrahedral sites and Be-O-Be bridges are avoided. The failure to synthesize sapphirine with more than 2 Be per formula unit of 40 O is consistent with a crystallographic constraint on maximum Be content (Christy et al. 2002).

* E-mail: esgrew@maine.edu

0003-004X/07/0001–80$05.00/DOI: 10.2138/am.2007.2250

Determining the cation distribution in welshite and how its high-Be content can be accommodated without Be-O-Be bridges required a single-crystal structure refinement. However, welshite is commonly polysynthetically twinned, and previous attempts to refine its structure have failed, most recently by Grew et al. (2001). New attempts led to successful refinement of the crystal structure of one mostly untwinned welshite sample, whereas the structure of a second, more extensively twinned sample could not be resolved entirely. The refinement established how unfavorable Be-O-Be bridges are avoided in welshite through symmetry reduction from $P\bar{1}$ to *P*1 (so far a unique symmetry class among the minerals of the aenigmatite-sapphirine-surinamite group), and how the *P*1 symmetry arises from charge ordering of the cations in sixfold and fourfold coordination. The present paper also presents new electron- and ion-microprobe data and Mössbauer spectroscopic data to understand better the crystal chemistry of this mineral.

Samples

Nine samples were selected for analyses (Table 1), including NRM040068 (originally PN) and NRM 850006 (originally NRM85006) studied by Grew et al. (2001) and the type specimen, NRM 532480, studied by Moore (1978). Welshite has been found only in the Långban deposit, Bergslagen, Sweden, where it typically occurs in dolomite and calcite in association with hematite, magnetite, and one or more silicates. Accompanying accessory minerals include one or more oxides with Sb^{5+}, and in most cases, one or more arsenates. A few samples contain swedenborgite, the only Be mineral occurring with welshite (Nysten et al. 1999).

Single-crystal X-ray diffraction of welshite

A dark-brown irregularly shaped fragment of welshite NRM040068 (approx. $0.12 \times 0.09 \times 0.07$ mm) was mounted on a Bruker-AXS diffractometer equipped with a Mo$K\alpha$ rotating anode generator and a SMART-1K area detector. The raw intensity data were processed with the SAINT software (Bruker 2000) and corrected for absorption with the SADABS program (Sheldrick 1996). The structure determination and refinement were carried out with the SHELX-97 package (Sheldrick 1997). Details of the data collection and refinement are summarized in Table 2.

The selected crystal of welshite NRM040068 yielded a triclinic unit cell typical of minerals of the aenigmatite-sapphirine-surinamite group (Table 2), but did not show any evidence of the twofold rotation twinning commonly found in these minerals, such as krinovite (Merlino 1972; Bonaccorsi et al. 1989), rhönite (Bonaccorsi et al. 1990), and høgtuvaite (Grew et al. 2005). However, crystals of other welshite samples that were examined (samples NRM 040069 and 900030) did indeed show the extra reflections characteristic of twinning. After unsuccessful attempts to solve the structure of welshite NRM040068 in the $P\bar{1}$ space group, the solution was obtained in the non-centrosymmetric *P*1 space group. The subsequent full structure refinement revealed the presence of only a very minor amount of chiral twinning in the crystal used (approximately 4 vol%, Table 2).

The structure determination was carried out on the basis of the chemical composition of welshite NRM040068 reported previously, viz., $^{VIII}[Ca_4]^{VI}[Mg_{7.6}Mn_{1.4}Sb_{3.0}]^{IV}[Si_{5.6}Be_{3.4}Fe_{1.26}Al_{1.4}As_{0.34}]O_{40}$ (Grew et al. 2001). The formula corresponds to 28 fully occupied cations sites and 40 O atoms per unit cell with Sb^{5+}, As^{5+}, Fe^{3+}, and Mn^{2+} oxidation states. After establishing that three octahedral sites and two tetrahedral sites were fully occupied by Sb and Be, respectively, the occupancies of the other cations sites were refined. A constraint of equal U_{eq} parameters for sites with the same coordination number was imposed initially and subsequently released after the occupancies had converged to stable values. It is worth pointing out that, because the *P*1 symmetry of welshite NRM040068 is mainly a result of its cation distribution, the refinement was found to be rather unstable until approximately correct site occupancies were determined. This

Table 1. Minerals associated with welshite in the Långban deposit, Sweden

NRM number	532480*	850006†	860108	900026	900027	900028	900030	040068†	040069
Former number		85006†						PN†	EJ
Be-Sb^{5+} minerals									
Welshite	A	A	A	A	A	A	A	A	A
Swedenborgite	A	–	–	–	–	–	–	A	–
Carbonates, oxides, silicates									
Dolomite	XX	XX	–	XX	X	XX	X	XX	–
Calcite	A	X	XX	XX	XX	XX	XX	X	XX
Hematite	XX	XX	XX	XX	XX	X	X	XX	XX
Magnetite	–	X	XX	XX	XX	XX	XX	XX	XX
Forsterite	–	X	X	X	–	–	–	–	–
Richterite	X	–	–	–	–	–	–	–	–
Phlogopite	X	X	X	X	–	X	–	–	XX
Lizardite	–	–	X	–	A	X	X	–	X
Arsenates									
Adelite	A	–	–	–	–	–	–	–	–
Berzeliite	A	A‡	A‡	–	A	A	A	–	A
Svabite	–	XX	–	–	–	–	–	–	–
Tilasite	–	X	–	–	A	–	XX	–	–
Other Sb^{5+} minerals									
Filipstadite	–	–	–	–	–	–	–	A	–
Ingersonite	–	–	–	–	–	–	–	A	–
Katoptrite	–	–	–	–	–	–	–	A	–
Roméite	A	A‡	A‡	A‡	A‡	A‡	A‡	–	A‡
Tegengrenite	–	–	–	–	–	–	–	A	–

Notes: XX = major constituent; X = subordinate constituent; A = accessory constituent.
* Type sample studied by Moore (1978).
† Studied by Grew et al. (2001). The tabulated phases have been identified by optical microscopy, powder XRD- and/or SEM/EDS-methods except those indicated by a double-dagger (‡), which were identified under the binocular microscope.

TABLE 2. Single-crystal X-ray refinement of welshite NRM040068

Space group	*P*1
a (Å)	10.394(3)
b (Å)	10.777(3)
C (Å)	8.896(2)
α (°)	105.953(4)
β (°)	96.294(4)
γ (°)	124.948(3)
V (Å)^3	738.8(3)
Z	1*
Calc. density (g/cm^3)	3.894
μ (mm^{-1}) (Mo*K*α)	5.281
2θ max (°)	72.62
h_{min}, h_{max}	–17, 13
k_{min}, k_{max}	–14, 17
l_{min}, l_{max}	–14, 10
Unique reflections	8048
Reflections [$I > 2\sigma(I)$]	7452
Absorption correction	SADABS program
T_{min}/T_{max}	0.7709
R_{int}	0.0414
Parameters refined	615
Chiral twinning parameter	0.037(19)
Weighting scheme	$w = 1/[\sigma^2(F_o^2) + (0.0103P)^2]$ where $P = (F_o^2 + 2F_c^2)/3$
Extinction expression	$F_c^* = kF_c [1 + 0.001 \times F_c^2\lambda^3/\sin 2\theta]^{-1/4}$
Extinction coefficient *x*	0.00529(19)
$R(F)$ [$I > 2\sigma(I)$]	0.0296
$wR(F^2)$ (8048 reflections)	0.0566
$\Delta\rho_{min}$ (e/Å^3)	–1.186
$\Delta\rho_{max}$ (e/Å^3)	1.683

* Simplified chemical formula for welshite NRM 040068 based on 28 cations and 40 O atoms $Ca_{3.78}Mg_{7.87}Sb_{3.00}Mn_{1.35}Si_{5.73}Be_{3.33}Al_{1.71}Fe_{0.96}As_{0.27}O_{40}$. $\Delta\rho_{min}$ and $\Delta\rho_{max}$ are the minimum and maximum residual electron densities in terms of electrons per cubic angstrom.

difficulty may explain the lack of success in previous attempts to refine the crystal structure. The final site occupancies yield uniform displacement parameters for all sites and are consistent with the average bond lengths. The corresponding chemical composition, viz. $^{VIII}[Ca_{3.78}Mn_{0.22}]^{VI}[Mg_{7.87}\ Sb_{3.00}\ Mn_{1.13}]^{IV}[Si_{5.73}\ Be_{3.33}Al_{1.71}Fe_{0.96}As_{0.27}]O_{40}$, is in good agreement with the analytical data (see below) considering that minor amounts of a third element possibly present in some sites have been ignored during the refinement.

All cation and oxygen sites were refined anisotropically in the final cycles of refinement. The final agreement indices are given in Table 2; the atomic coordinates and equivalent isotropic displacement parameters in Table 3;[1] the anisotropic displacement parameters in Table 4a;[1] the site occupancies, average bond lengths and calculated electrostatic site potentials in Table 4b; selected bond lengths and selected tetrahedral chain bond angles in Table 4c.[1]

Attempts to refine the structure of NRM900030 were foiled by the presence of about 25% of rotation twinning plus some chiral twinning, which SHELXL is unable to handle simultaneously. By adjusting the individual site occupancies through trial and error based on the U parameters, and by ignoring any chiral twinning present, the structure could be refined to $wR(F^2) = 15.4\%$ for 22713 reflections [$R(F) = 6.2\%$ for 16411 reflections with $F > 4\sigma(F)$] with good e.s.d.values on bond distances and angles. There is no doubt that welshite 900030 also crystallizes with *P*1 symmetry. However, because this symmetry is the direct result of cation ordering, strong correlations between the site occupancies, and the amount of chiral twinning made the refinement unstable. Only the mixed occupancies of the three M sites containing Sb and Fe converged properly, yielding a much lower Sb content (1.64 Sb per 40 O) than for welshite NRM040068 (3 Sb per 40 O). The major difference between NRM040068 and NRM900030 appears to be less cation/charge ordering in the latter, likely as a result of the smaller Sb content.

Unit-cell parameters have been measured for crystal fragments extracted from the three welshite samples examined in this work, NRM040068, -040069, and -900030 (Table 5). Unit-cell edges (with one exception) and volume increase with increasing Sb and decreasing Fe^{3+} and Si. These variations are consistent with the coupled substitutions involving the octahedral and tetrahedral sites, $^{VI}Sb^{5+} + {}^{VI}Mg^{2+} + {}^{IV}Fe^{3+} = 2\ {}^{VI}Fe^{3+} + {}^{IV}Si^{4+}$ (see below), and with the corresponding ionic radii (Shannon 1976).

CATION DISTRIBUTION IN WELSHITE NRM040068

Part of the structure of welshite NRM040068 is shown in Figure 1. The geometry of the structure is very similar to that of other minerals of the aenigmatite-sapphirine-surinamite group and the main structural features have been described previously, e.g., for rhönite (Bonaccorsi et al. 1990). The emphasis of the present discussion will be on the unique cation distribution found in welshite and its relationship to the chemical composition.

The absence of a center of symmetry in welshite NRM040068 is associated with the splitting of most cation and anion sites in the unit cell, with pairs of sites (e.g., T1-T1A, M3-M3A, O1-O1A etc.) related by a pseudo-inversion operation (Table 3). As a result, ordering of cations in fourfold and sixfold coordination becomes possible without the formation of a superstructure, as for instance, observed previously in khmaralite (Barbier et al. 1999). No strong ordering occurs on the four Ca-dominated sites (M8, M9, M8A, M9A—Table 4b) although their coordinations differ as allowed by the P1 symmetry (CN = 8 for M8A/M9A vs. CN = 7+1 for M8/M9). The different distortions could probably be linked to the tetrahedral ordering. Overall, the cation distribution is driven by charge ordering on both the octahedral (M) and tetrahedral (T) sites. This is supported by the calculation of electrostatic site potentials (Table 4b), which shows that the refined cation distribution is self-consistent: the highly charged Sb^{5+} cations are fully ordered on the three M sites with large negative potentials (average of –48.7 V for M7, M3A, and M4A) while the Be^{2+} cations are preferentially ordered on the T sites with the least negative potentials (average of –32.9 V for T4, T1A, and T2A).

As in all other Be-containing minerals of the aenigmatite-sapphirine-surinamite group (sapphirine, khmaralite, makarochkinite, høgtuvaite, surinamite), the Be cations are found to occupy some of the most polymerized T sites that share corners with three other T sites. However, due to the absence of an inversion center in welshite, the T4 and T1A sites (100% Be) are crystal-

[1] Deposit item AM-07-002, Tables 3, 4a, and 4c (atomic coordinates, displacement parameters, and site occupancies and other data). Deposit items are available two ways: For a paper copy contact the Business Office of the Mineralogical Society of America (see inside front cover of recent issue) for price information. For an electronic copy visit the MSA web site at http://www.minsocam.org, go to the American Mineralogist Contents, find the table of contents for the specific volume/issue wanted, and then click on the deposit link there.

TABLE 4B. Cation site occupancies*, average bond lengths (Å) and electrostatic site potentials (V) in welshite NRM040068

Site	%Mg	%Mn	%Sb	%Ca	<M-O>	Electrostatic Potential†	Site	%Be	%Si	%As	%Al	%Fe	<T-O>	Electrostatic Potential†
M1	87	13	–	–	2.075	–25.45	T1	–	100	–	–	–	1.630	–48.45
M2	92	8	–	–	2.081	–25.20	T2	–	99	1	–	–	1.635	–49.26
M3	95	5	–	–	2.105	–25.34	T3	52	–	–	48	–	1.718	–33.70
M4	94	6	–	–	2.114	–25.30	T4	100	–	–	–	–	1.636	–33.02
M5	66	34	–	–	2.161	–24.20	T5	–	–	–	48	52	1.843	–33.64
M6	64	36	–	–	2.160	–24.57	T6	–	87	13	–	–	1.653	–49.05
M7	–	–	100	–	1.982	–49.02	T1A	100	–	–	–	–	1.650	–32.60
M8	–	11	–	89	2.444	–22.21	T2A	81	–	–	19	–	1.682	–32.99
M9	–	3	–	97	2.451	–22.18	T3A	–	97	3	–	–	1.642	–48.98
M3A	–	–	100	–	1.991	–48.29	T4A	–	100	–	–	–	1.624	–49.01
M4A	–	–	100	–	1.987	–48.71	T5A	–	90	10	–	–	1.651	–48.84
M5A	91	9	–	–	2.121	–24.89	T6A	–	–	–	56	44	1.829	–33.92
M6A	98	2	–	–	2.077	–24.47								
M7A	100	–	–	–	2.085	–24.97								
M8A	–	–	–	100	2.472	–21.39								
M9A	–	8	–	92	2.472	–22.02								

* The standard uncertainties on site occupancies were 0.4% for Mg/Mn, 0.3% for Si/As and Fe/Al, and 0.9% for Be/Al. The small amounts of Mn on the M8, M9, M8A, and M9A sites were adjusted by inspection of the U_{eq} parameters. The overall composition is $Ca_{3.78}Mg_{7.87}Sb_{3.00}Mn_{1.35}Si_{5.73}Be_{3.33}Al_{1.71}Fe_{0.96}As_{0.27}O_{40}$.
† The potentials were calculated by the Bertaut method with a program written by Y. Ohashi and provided by J. Smyth of the University of Colorado (Smyth 1989). The potentials for the O sites range from +25.49 V to +28.78 V.

TABLE 5. Unit-cell parameters of welshite measured by single-crystal X-ray diffraction

Sample NRM-	*a* (Å)	*b* (Å)	*c* (Å)	α (°)	β (°)	γ (°)	*V* (Å³)
040068	10.394(3)	10.777(3)	8.896(2)	105.953(4)	96.294(4)	124.948(3)	738.8(6)
040069*	10.377(6)	10.769(7)	8.880(5)	105.77(2)	96.35(2)	125.03(1)	735.8(13)
040069*	10.365(2)	10.730(2)	8.895(2)	105.82(3)	96.55(3)	124.97(3)	732.7(15)
900030	10.345(1)	10.727(1)	8.841(1)	105.663(1)	96.362(1)	125.035(1)	728.2(1)

* Crystals of welshite 040069 were of poorer quality. The parameters measured on different crystals suggest chemical heterogeneity.

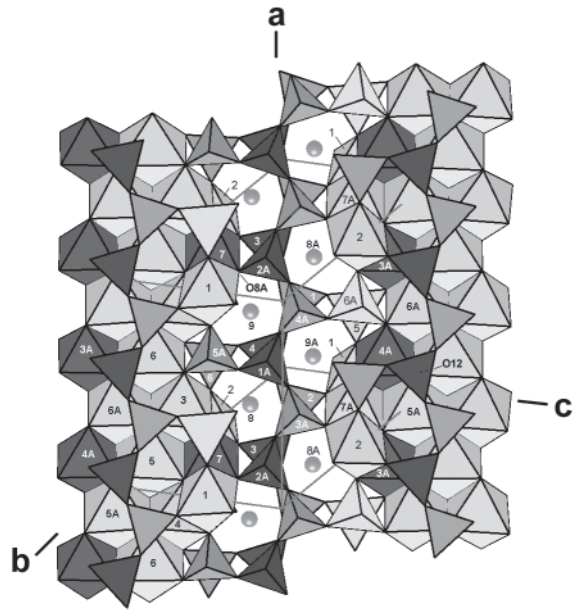

FIGURE 1. View of the welshite structure approximately along the [122] direction of the triclinic unit cell. The cation sites are labeled as in Table 4b. Dark gray = Sb octahedra and Be-rich tetrahedra; medium gray = Si-rich tetrahedra, light gray = Mg/Mn octahedra and Al/Fe tetrahedra.

lographically distinct from the T4A and T1 sites (100% Si) and a nearly complete Be/Si ordering becomes possible along the backbone of the tetrahedral chains (Fig. 1). Indeed, the *P*1 symmetry allows the structure to accommodate the large Be content of welshite (3.33 Be per 40 O atoms) by including several T sites with 100% Be occupancies without the formation of unfavorable tetrahedral Be-O-Be linkages, as previously envisaged (Grew et al. 2001). Such T-site ordering is not possible in aenigmatite-type structures with $P\bar{1}$ symmetry and this observation had led to the earlier proposal of a maximum content of 2 Be per 40 O atoms in beryllian sapphirines (Christy et al. 2002).

Coupled ordering of cations in fourfold and sixfold coordination is shown by the fact that the three M sites containing 100% Sb^{5+} predominantly share corners with either Be/Al or Al/Fe T sites, rather than with Si-rich T sites (Fig. 1). Only two such linkages are present in the structure, viz. M3A-O5A-T5A and M4A-O16-T6, in which oxygen overbonding is avoided by lengthening the T-O bonds significantly (1.716 Å for T5A-O5A and 1.717 Å for T6-O16—Tables 4b and 4c). The presence of the highly charged Sb^{5+} cation in the M7 site is analogous to that of Ti^{4+} cations in the M7 site of other minerals of the aenigmatite-sapphirine-surinamite group, including aenigmatite (Cannillo et al. 1971), rhönite (Bonaccorsi et al. 1990), and makarochkinite (Grew et al. 2005). However, the generally lower Ti content of these minerals yields only a partial Ti occupancy of the M7 site, viz., 59% Ti for a makarochkinite sample from the Il'men Mountains in Russia (Grew et al. 2005). The much larger Sb content of welshite (3.0 Sb per 40 O atoms) is equivalent to a full 100% Sb occupancy in three octahedral sites. The complete ordering of the Sb^{5+} cations in M7, M3A and M4A is not only consistent with the strongly negative electrostatic potentials calculated for these sites (Table 4b) but also avoids edge sharing between SbO_6 octahedra (Fig. 1). The latter may actually impose an upper limit of 3 Sb atoms per unit-cell when combined with the Be and Si distributions and the need to minimize corner sharing between SbO_6 octahedra and Si-rich tetrahedra. The larger Sb content proposed for an end member welshite composition of $Ca_4Mg_8Sb_4O_4[Si_6Be_6O_{36}]$ (Hawthorne and Huminicki 2002) is possible from the point of view of avoiding edge sharing between SbO_6 octahedra (with 100%

Sb occupancies for M3, M4, M3A, M4A) but is unlikely since it would necessarily involve multiple corner sharing between SbO_6 octahedra and SiO_4 tetrahedra. Overall, the large Sb^{5+} content of welshite provides the required charge compensation for the large Be^{2+} content and the associated 100% Sb and 100% Be occupancies of several M and T sites, respectively, clearly define welshite as a unique member of the aenigmatite-saphirine-surinamite group of minerals (see below).

As expected, if charge ordering is the main driving force behind the cation distribution in welshite, no strong Mg/Mn ordering is observed in the remaining M sites (Table 4b). The analytical chemical composition (see below) indicates that a minor amount of Fe must be present on the octahedral sites as well. However, Fe and Mn cannot be determined independently from X-ray diffraction data and the minor octahedral Fe content has been assimilated to Mn during the refinement of site occupancies. Mössbauer spectroscopy data indicate that a small fraction of Fe^{3+} should be present on the octahedral M sites. This finding is consistent with the observed M-O bond distances and the electrostatic potentials (Tables 3 and 4b): the M1-4 sites, with one or more short M-O bonds and with slightly more negative site potentials, could well contain minor amounts of smaller and more highly charged Fe^{3+} cations.

MÖSSBAUER SPECTROSCOPY

Method

^{57}Fe Mössbauer spectra were obtained on three of the present samples (NRM040068, -040069, and -900030). Absorbers were prepared from separated welshite crystals by pressing finely ground samples between mylar windows in a 2.5 mm circular aperture of a Pb-disk. The absorber thickness ranged from 1 to 2 mg Fe/cm^2. Spectra were collected at room temperature using a conventional spectrometer system operated in constant acceleration mode with a nominal 10 m Ci ^{57}Co/Rh point source. Spectral data for the velocity range –4.5 to 4.5 mm/s were recorded in a multichannel analyzer using 1024 channels. After velocity calibration against room temperature α-Fe foil spectra, raw spectrum data were folded and fitted using the MDA least-square fitting program (Jernberg and Sundqvist 1983) assuming Lorentzian peak shapes and equal width and intensity of the two components of each fitted quadrupole doublet.

Fe valency and distribution

The recorded Mössbauer spectra of welshite (Fig. 2) comprise one strong absorption doublet in the range –0.5 to 1.0 mm/s and, in two spectra, a very weak absorption at ca 2.5 mm/s. The strong central doublet reveals variable asymmetry and also peak width indicating that more than one quadrupole doublet contributes to this absorption. All three obtained spectra could be well fitted with a maximum of three quadrupole doublets. Application of fitting models with larger number of quadrupole doublets resulted in only very marginally improved χ^2-values. The hyperfine parameters and relative intensities of the fitted doublets are summarized in Table 6.

Two fitted intense quadrupole doublets with center shifts of ca. 0.2 and 0.4 mm/s are due to Fe^{3+} at tetrahedral sites and octahedral sites, respectively. The doublet of very low intensity observed in two of the samples displays a center shift (ca. 1.1 mm/s) commonly observed for Fe^{2+} at six-coordinated sites (e.g., Coey 1984).

The relatively large widths of the fitted quadrupole doublets (Table 6) are likely due to a combination of causes. First, the point source used increases the width slightly (ca. 0.02 mm/s) in relation to a conventional source. Second, as evidenced by the present structure refinement of welshite, the Fe cations are distributed over several octahedral and tetrahedral sites, which display different mean bond lengths and distortions from ideal O_h- and T_d-symmetry. In addition, the Mössbauer spectra were recorded on milligram-sized "bulk samples" of welshite, which our electron microprobe analyses show to be heterogeneous on a fine scale, particularly in NRM900030.

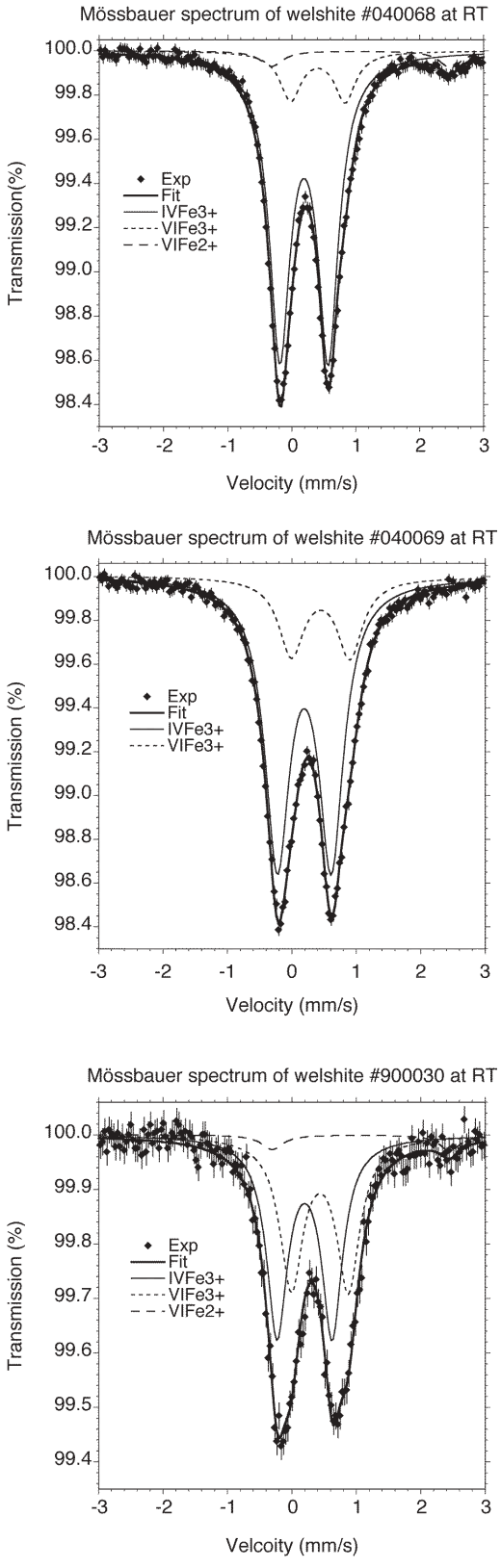

FIGURE 2. Room-temperature Mössbauer spectra of three welshite samples.

In summary, the Mössbauer spectra show that Fe^{3+} is overwhelmingly dominant: $Fe^{3+}/Fe_{tot} = 0.96–1.00$. Ferric iron is dominantly tetrahedral in welshite containing ~3 Sb/40 O, but the proportion of octahedral Fe^{3+} increases with decreasing Sb-content (see below).

Chemical composition of welshite

Methods of electron and ion microprobe analysis

Welshite grains from the present samples were analyzed for heavier elements ($Z \geq 9$) on a Cameca SX50 electron microprobe operating at an acceleration voltage of 20 kV and a sample current of 12 nA, in the Earth Sciences Department, Uppsala University. Standard samples comprised synthetic MgO (Mg), Fe_2O_3 (Fe), Al_2O_3 (Al), ZnS (Zn), $CaSiO_3$ (Ca and Si), $MnTiO_3$ (Mn and Ti), Sb_2S_3 (Sb), and AsGa (As), and natural albite (Na) and orthoclase (K). For raw data reduction, the PAP computer program was applied (Pouchou and Pichoir 1984).

Secondary ion mass spectrometry (SIMS) was conducted on gold-coated polished thin sections using a Cameca ims 4f ion microprobe at the University of New Mexico. Analyses were made using primary $^{16}O^-$ ions accelerated through a nominal potential of 10 kV. Lithium was analyzed separately with a $^{16}O^-$ ions accelerated through a nominal potential of 12.5 kV. In all analyses, a primary beam current of 10 nA was focused on the sample over a spot diameter of 10–15 µm. Sputtered secondary ions were energy-filtered using a sample offset voltage of 50 V, energy window of ±25 V. In mineral matrices with high Be and relatively low Al (i.e., welshite), a mass resolution of ~320 (routine operating conditions) was sufficient to measure $^9Be^+$. Acquisition times for 10 counting cycles at each spot were 4 s ($^7Li^+$), 5 s ($^9Be^+$), 10 s ($^{11}B^+$), and 6 s ($^{30}Si^+$). The analytical procedure included counting on a background position to monitor detection noise.

Absolute concentrations of each element were calculated using empirical relationships of measured $^9Be^+/^{30}Si^+$, $^7Li^+/^{30}Si^+$, and $^{11}B^+/^{30}Si^+$ ratios (normalized to known SiO_2 content). The light element concentrations in the unknowns were derived from working curves constructed from plots of SiO_2 wt% × $^9Be^+/^{30}Si^+$, $^7Li^+/^{30}Si^+$, or $^{11}B^+/^{30}Si^+$ count ratio vs. ppm element or wt% oxide of Li, Be, or B in standards. Because no standard even approaches welshite in composition, we used NRM040068 welshite as a Be standard because its Be/Si ratio had been determined by crystal-structure refinement. Grew et al. (2001) used makarochkinite, which gave a Be/Si = 0.566–0.590 for NRM040068, in good agreement with the crystal-structure refinement Be/Si ratio of 0.581. For Li and B standards, we used three synthetic doped granitic glasses prepared by J. Evensen (e.g., Evensen and London 2002, 2003) and NBS standard glasses 610 and 612, as well as three tourmalines (Dyar et al. 2001) for Li only. The glass and tourmaline standards gave different calibrations for Li, y = 0.0064x vs. y = 0.0054x, respectively. The tourmaline-based calibration was applied to welshite because it gave a better Li content for a prismatine used as an internal standard. Stripping the carbon coat, which is a potential source of B contamination, and carefully cleaning the surface prior to applying the gold coat to the sections, reduced the problem with B contamination of the section surface. As a result, B contents obtained in the present study do not exceed 7 ppm (Table 7) and are lower than those reported by Grew et al. (2001) for NRM850006 (2 vs. 17 ppm, Table 7) and NRM040068 (0.9 vs. 7 ppm). Nonetheless, the Li and B contents are undoubtedly much less accurate than Be contents because of the large difference in matrix between standards and welshite.

The ±10% reproducibility Grew et al. (2006) estimated for BeO as a major constituent is probably valid for welshite BeO contents. However, the precision for Li and B is expected to be much less because of their much lower contents.

Table 6. Mössbauer hyperfine parameters and intensities at room temperature

	CS mm/s	DQ mm/s	w mm/s	I %
Welshite NRM040068 ($\chi^2 = 1.505$)				
$^{VI}Fe^{2+}$	1.08	2.79	0.41	04(2)
$^{VI}Fe^{3+}$	0.40	0.85	0.40	14(2)
$^{IV}Fe^{3+}$	0.19	0.76	0.39	82(2)
Welshite NRM040069 ($\chi^2 = 1.005$)				
$^{VI}Fe^{3+}$	0.44	0.90	0.48	22(2)
$^{IV}Fe^{3+}$	0.19	0.84	0.46	78(2)
Welshite NRM900030 ($\chi^2 = 1.094$)				
$^{VI}Fe^{2+}$	1.07	2.75	0.39	04(4)
$^{VI}Fe^{3+}$	0.43	0.88	0.43	44(4)
$^{IV}Fe^{3+}$	0.20	0.85	0.39	52(4)

Notes: CS = centroid shift; DQ = quadrupole splitting; w = full width at half maximum; I = intensity. Estimated error of Mössbauer hyperfine parameters is 0.02; estimated errors for intensities given in parentheses.

Compositional variations and substitution mechanisms

Constituents invariably present in welshite are BeO, MgO, Al_2O_3, SiO_2, CaO, MnO, total Fe as Fe_2O_3, As_2O_5, and Sb_2O_5, whereas Na_2O, TiO_2, and ZnO appear erratically in the analyses (Table 7). Lithium is more abundant than B, but unlike B, it has received little attention as a constituent of minerals from Långban; we are aware of only one other report of Li analyses (Engström 1874). Back-scattered electron (BSE) images of the analyzed grains reveal compositional heterogeneity in the relatively heavy constituents Sb and Fe, which reaches an extreme in NRM 900030 (Figs. 3 and 4). Moreover, Li contents are variable in a given sample: 33 vs. 56 ppm (Table 7) for NRM850006; 6.5–8.7 ppm (Grew et al. 2001) vs. 1 ppm (Table 7) for NRM040068.

The analyzed samples can be divided into two distinct groups (Fig. 5): (1) compositions with ~3 Sb/40 O, and (2) compositions with <3 Sb/40 O. The composition of the crystal of 040069 studied by X-ray diffraction (040069 xrd in Fig. 5) plots between the compositions of the two types, and could represent a transitional type. Si varies inversely with Sb as in type 2, but along a different trend, whereas Fe contents are higher and Sb contents slightly lower than corresponding contents in type 1. The coupled substitution proposed by Grew et al. (2001) on the basis of NRM 040068 and NRM 850006, $0.59^{VI,IV}(Fe,Al)^{3+} \approx 0.42^{VI}(Mg,Mn,Fe)^{2+} + 0.21(^{VI}Sb,^{IV}As)^{5+}$, could not be confirmed in either group.

Most of the samples belong to the first group, which is typified by the sample for which the structure was refined successfully, NRM040068. The structure refinement gives Si + As = 6, and the EMPA data on the samples in group 1 appear to obey this relationship, albeit with considerable scatter (Fig. 6). Inverse variation of Al with Fe^{3+} extends over a much wider range (Fig. 7). This one-to-one inverse variation can be attributed to homovalent Al-Fe substitution on T sites. Horizontal displacement could be due either to variable Be content or to variable ^{VI}Fe content. Deducting ^{VI}Fe from two samples analyzed by Mössbauer spectroscopy results in close approximation of $^{IV}(Fe + Al + Be) = 6$, i.e., the samples plot close to the line for Be measured by SIMS in these samples. Addition of ^{VI}Fe determined by Mössbauer to Mg + Mn gives an average of 13 cations, i.e., 9 cations for the M1-M6 and M5A-M7A sites in these two samples. Thus a generalized and simplified formula for the group 1 welshite compositions is $(Ca,Mn)_4(Mg,Mn,Fe^{3+})_9Sb_3(Si,As)_6(Be,Al)_4(Al,Fe^{3+})_2O_{40}$, which can be idealized to a mixture of Al and Fe analogs, respectively $Ca_4Mg_9Sb_3Si_6Be_3Al_3O_{40}$ and $Ca_4Mg_9Sb_3Si_6Be_3AlFe_2O_{40}$. The Al analog is exactly intermediate between two end-members proposed by Hawthorne and Huminicki (2002), respectively $Ca_4Mg_8Sb_4Si_6Be_6O_{40}$ and $Ca_4Mg_{10}Sb_2Si_6Al_6O_{40}$ (Table 8). We suggest that $Ca_4Mg_9Sb_3Si_6Be_3Al_3O_{40}$ and $Ca_4Mg_9Sb_3Si_6Be_3AlFe_2O_{40}$ are more appropriate end-members for group 1 welshite.

Sample 900030 and the crystal of NRM850006 studied by Grew et al. (2001) are type 2. Crystals of NRM900030 are markedly zoned on very fine scale (e.g., Figs. 3 and 4). The intensity of back-scattered electrons closely tracks the Sb content,

TABLE 7. Selected electron and ion microprobe analyses of welshite

Sample NRM-	040068*	040068†	040069†	040069*	900026*	900027*	900028*	532480*	850006*	850006*	860108*	900030†	900030†	900030†
Analysis	SREF§	Ave‡	Single	Ave‡	Single	Single	Single	Single	Single	Single	Single	Single	Single	Ave‡
Note				xrd xl					1‖	2‖		dark	light	xrd xl
wt%														
SiO_2	19.87	18.93	19.45	19.15	18.49	19.61	19.04	19.55	19.38	19.21	19.40	24.00	21.07	23.20
TiO_2	–	0.01	0.12	0.00	0.11	0.12	0.08	0.00	0.00	0.29	0.07	0.18	0.24	0.07
Al_2O_3	5.03	4.44	3.01	1.83	3.72	7.26	3.29	3.29	2.92	5.33	5.09	1.49	1.43	1.66
Fe_2O_3	4.42	5.65	8.97	13.06	9.75	3.02	10.20	9.22	14.02	6.67	7.09	21.79	17.10	20.73
FeO	–	0.21	0.00	–	–	–	–	–	–	–	–	0.82	0.64	0.78
MgO	18.31	17.88	20.13	18.04	18.81	19.28	18.86	19.35	17.42	18.52	19.95	16.11	16.57	16.76
MnO	5.53	4.71	0.60	0.81	0.98	3.13	0.56	0.78	1.14	1.95	0.66	1.47	0.92	1.26
ZnO	–	0.16	0.00	0.16	0.02	0.55	0.00	0.31	0.00	0.16	0.00	0.12	0.00	0.06
Sb_2O_5	28.01	27.76	27.34	24.60	25.31	27.54	26.31	27.24	23.16	27.39	27.03	14.05	19.53	15.61
As_2O_5	1.79	2.43	2.54	2.70	4.04	2.30	3.49	2.49	3.58	2.00	2.21	2.59	3.31	2.70
CaO	12.23	12.08	12.50	12.55	12.58	11.92	12.76	12.28	12.96	12.54	12.39	12.60	12.65	12.67
Na_2O	–	0.01	0.12	0.00	0.00	0.28	0.11	0.22	0.00	0.01	0.18	0.20	0.12	0.17
K_2O	–	0.00	0.00	0.00	0.00	0.00	0.00	0.00	0.00	0.00	0.00	0.00	0.00	0.00
BeO#	4.81	4.58	4.63	4.63	4.72	3.98	4.81	4.43	4.99	4.60	4.42	4.96	4.94	4.81
Sum	100.00	98.85	99.43	97.54	98.54	99.00	99.52	99.18	99.58	98.69	98.48	100.39	98.43	100.48
ppm														
Li**	–	1	57	57	21	29	18	160	33	56	10	11	11	11
B**	–	0.9	3	3	0.7	1	1	3	1.5	1.5	1	6	6	7
Formula per 40 O														
Si	5.73	5.570	5.621	5.677	5.389	5.657	5.500	5.678	5.586	5.579	5.614	6.687	6.091	6.494
As	0.27	0.374	0.384	0.418	0.616	0.348	0.528	0.379	0.540	0.303	0.334	0.377	0.500	0.395
Al	1.71	1.539	1.025	0.639	1.278	2.468	1.120	1.128	0.992	1.823	1.736	0.489	0.487	0.548
Be	3.33	3.237	3.211	3.294	3.307	2.761	3.336	3.091	3.459	3.208	3.069	3.318	3.434	3.233
Fe^{3+}	0.96	1.068	1.522	1.971	1.410	0.656	1.516	1.725	1.423	1.087	1.247	1.129	1.489	1.331
Sum T cations	12.000	11.789	11.763	12.000	12.000	11.890	12.000	12.000	12.000	12.000	12.000	12.000	12.000	12.000
Sb	3.00	3.034	2.935	2.709	2.740	2.951	2.823	2.939	2.480	2.954	2.904	1.453	2.098	1.623
Fe^{3+}	0.00	0.182	0.429	0.943	0.729	0.000	0.700	0.290	1.618	0.371	0.296	3.439	2.232	3.035
Ti	–	0.002	0.026	0.000	0.024	0.025	0.018	0.000	0.000	0.063	0.015	0.037	0.053	0.016
Fe^{2+}	–	0.052	0.000	–	–	–	–	–	–	–	–	0.190	0.155	0.182
Mg	7.87	7.842	8.674	7.972	8.173	8.292	8.123	8.380	7.486	8.018	8.603	6.690	7.143	6.992
Mn	1.35	1.173	0.147	0.203	0.241	0.766	0.138	0.193	0.278	0.481	0.161	0.348	0.225	0.300
Zn	–	0.035	0.000	0.035	0.004	0.118	0.000	0.066	0.000	0.035	0.000	0.025	0.000	0.012
Ca	3.78	3.808	3.871	3.986	3.930	3.685	3.951	3.822	4.003	3.900	3.842	3.761	3.918	3.799
Na	–	0.003	0.070	0.000	0.000	0.156	0.064	0.126	0.000	0.008	0.101	0.111	0.065	0.094
K	–	0.001	0.000	0.000	0.000	0.000	0.000	0.000	0.000	0.000	0.000	0.001	0.000	0.000
Li	–	0.000	0.014	0.015	0.005	0.007	0.005	0.040	0.008	0.014	0.003	0.003	0.003	0.003
Sum M cations	16.000	16.133	16.166	15.863	15.847	16.000	15.822	15.857	15.872	15.844	15.925	16.058	15.891	16.055
Sum cations	28.000	27.922	27.929	27.863	27.847	27.890	27.822	27.857	27.872	27.844	27.925	28.058	27.891	28.055

Notes: Wt% sums include Li as Li_2O.
* Fe assumed to be Fe_2O_3 and Fe assumed to fill the tetrahedral sites first.
† Fe valence and occupancy determined on a bulk sample by Mössbauer spectroscopy, except sample 900030, where Fe^{3+} is assumed to fill the tetrahedral sites first.
‡ Average of 6–8 points (electron microprobe only).
§ Single-crystal structure refinement.
‖ Sample 850006: 1 refers to one of three analyses averaged by Grew et al. (2001), 2 to a newly analyzed crystal.
Averages by ion microprobe (except single points for 900030 dark and light). BeO in sample NRM 040068 was done by SREF. BeO in sample NRM 040069 xrd was assumed to be the same as in the other crystals of this sample. BeO in NRM900030 xrd xl is an average of ion probe data on the other analyzed crystal of this sample. BeO in 860005-1 was calculated using 040068 as a standard from data reported in Grew et al. (2001).
** Averages by ion microprobe (except single points for B in 900030 dark and light). Li and B in sample NRM 040069 xrd were assumed to be the same as in the other crystals of this sample. Li and B in NRM900030 xrd xl is an average of ion probe data on the other analyzed crystal of this sample. Li in 860005-1 was taken from Grew et al. (2001); B in this sample assumed to be the same as in the other crystals.

which increases with ^{VI}(Mg,Mn), but decreases with Fe and Si (Fig. 8). The resulting net substitution, $Sb^{5+} + Mg^{2+} = Fe^{3+} + Si^{4+}$, although balanced in charge, must result from coupling of several substitutions because neither Sb nor Mg (Mn) occupy tetrahedral sites. A substitution balanced in site occupancy is $^{M}Sb^{5+} + {}^{VI}Mg^{2+} + {}^{IV}Fe^{3+} = {}^{M}Fe^{3+} + {}^{VI}Fe^{3+} + {}^{IV}Si^{4+}$, where M refers specifically to the M7, M3A, and M4A octahedral sites. Variations in Sb, Fe, and (Mg + Mn) corrected for Mn replacing Ca on the M8, M8A, M9, and M9A sites approach the ideal trends predicted by this substitution. Variations in Be, Al, and As are subordinate. Decreasing Sb should result in decreasing $^{IV}Fe/^{VI}Fe$ ratio (Fig. 9). Mössbauer spectra give $^{IV}Fe/^{VI}Fe = 1.2$ for a bulk sample of 900030 vs. 3.5–5.6 for bulk samples of NRM040068 and NRM040069 (Table 6). However, a ratio of 1.2 ± 0.2 is higher than predicted for a bulk composition of the points analyzed

TABLE 8. Welshite end-members

End-member	Source
$Ca_4Mg_8Fe^{3+}{}_2Sb_2O_4[Si_8Be_4O_{36}]$	Moore (1978), Strunz and Nickel (2001)
$Ca_4Mg_8Sb_4O_4[Si_4Be_4Al_4O_{36}]$	Hawthorne and Huminicki (2002)
$Ca_4Mg_8Sb_4O_4[Si_6Be_6O_{36}]$	Hawthorne and Huminicki (2002)
$Ca_4Mg_{10}Sb_2O_4[Si_6Al_6O_{36}]$	Hawthorne and Huminicki (2002)
$Ca_4Mg_{10}Sb_2O_4[Si_8Be_2Al_2O_{36}]$	Hawthorne and Huminicki (2002)
$Ca_4Mg_9Sb_3O_4[Si_6Be_3Al_3O_{36}]$	Type 1, this paper
$Ca_4Mg_9Sb_3O_4[Si_6Be_3AlFe_2O_{36}]$	Type 1, this paper
$Ca_4Mg_{8.55}Fe_{0.45}Sb_{3.0}O_4[Si_{5.15}As_{0.45}Be_{3.45}Al_{0.5}Fe_{2.45}O_{36}]$	Type 2, this paper
$Ca_4Mg_{7.05}Fe_{3.45}Sb_{1.5}O_4[Si_{6.65}As_{0.45}Be_{3.45}Al_{0.5}Fe_{0.95}O_{36}]$	Type 2, this paper

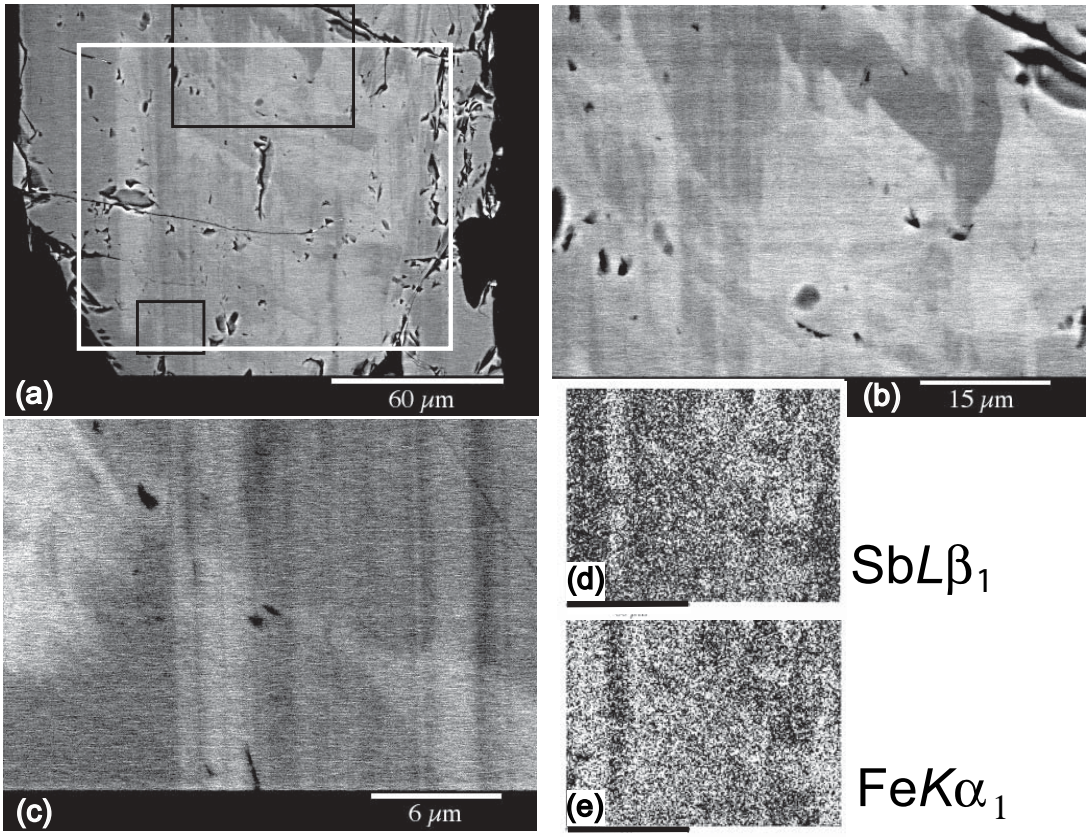

FIGURE 3. Images of sample 900030. (**a**) Small-scale back-scattered electron image of one crystal; large and small black rectangles outline the enlargements in **b** and **c**, respectively. (**d**) and (**e**) are Sb and Fe maps, respectively, of the area enclosed in white rectangle in **a**. Bars are 60 μm long.

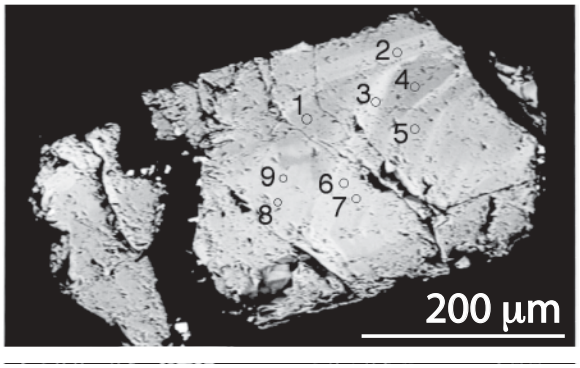

FIGURE 4. Back-scattered electron image of crystal from sample 900030 analyzed by electron and ion microprobes. Labeling of points in Figure 8 is: 1 and 4 = dark, 2 and 5 = medium, and 3, 6, 7, 8, and 9 = light.

by electron microprobe in a single crystal from the lot used for Mössbauer spectroscopy. This discrepancy could reflect differences in sampling and resolution, and for this reason, the Mössbauer data were not used to calculate Fe^{3+} occupancy in Table 7. Mössbauer spectroscopy is a bulk method needing several mg of sample, i.e., a large number of single welshite crystals, whereas the electron microprobe is a high-resolution method allowing analyses on the scale of fractions of a nanogram on a single crystal. Consequently, Mössbauer spectroscopy could have

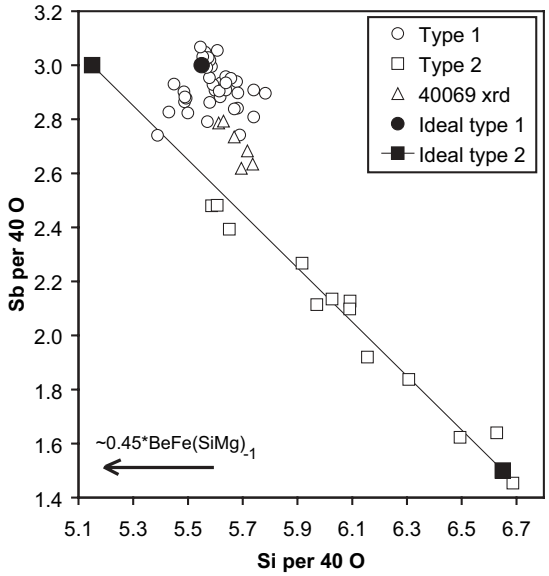

FIGURE 5. Plot of welshite compositions in terms of Sb and Si. Ideal end-member composition for type 1 gives Si content for 0.45 As per 40 O, the average As content of type 2. The arrow indicates the amount of the exchange ~0.45 × ($^{IV}Be + {}^{VI}Fe^{3+}$)($^{IV}Si + {}^{VI}Mg)_{-1}$ needed to relate the ideal compositions of types 1 and 2 at Sb = 3/40 Ox.

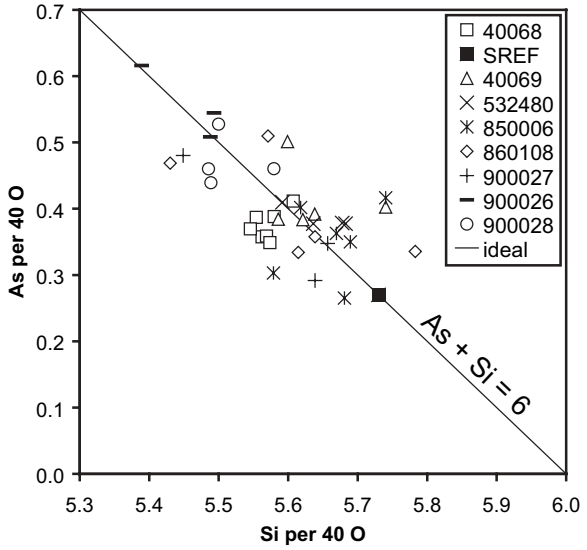

FIGURE 6. Plot of type 1 welshite compositions in terms of As and Si contents per formula unit. SREF refers to composition of 040068 determined by single-crystal structure refinement.

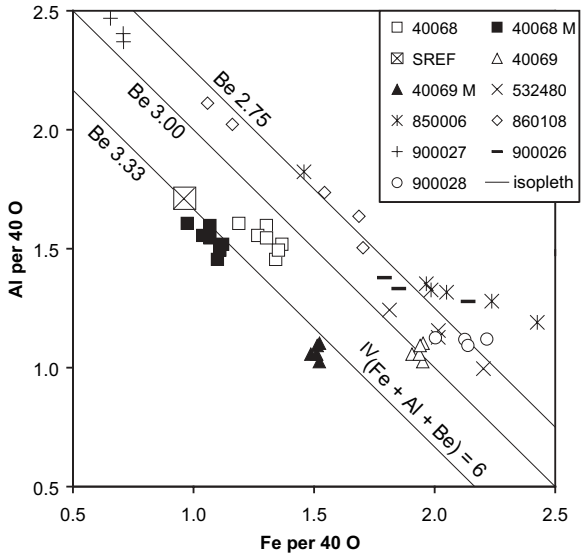

FIGURE 7. Plot of type 1 welshite compositions in terms of Al and total Fe per formula unit. SREF refers to composition of 040068 determined by single-crystal structure refinement. The suffix M indicates that only the $^{IV}Fe^{3+}$ determined by Mössbauer spectroscopy is plotted. The lines indicate the ideal relationship between Al and $^{IV}Fe^{3+}$ for the amount of Be per formula unit indicated and for As + Si = 6.00 per formula unit.

averaged over a wider range of composition than was analyzed with the electron microprobe.

Silicon contents in the Sb-poor crystal of 850006 lie along the trend set by sample 900030, whereas Fe^{3+} and ^{VI}(Mg,Mn) deviate slightly (Fig. 8). This crystal contains about twice as much Al as 900030, so part of the deviation could be due to Al = Fe^{3+} substitution at the T sites, as well as to unmeasured Fe^{2+}, which was not determined in 850006.

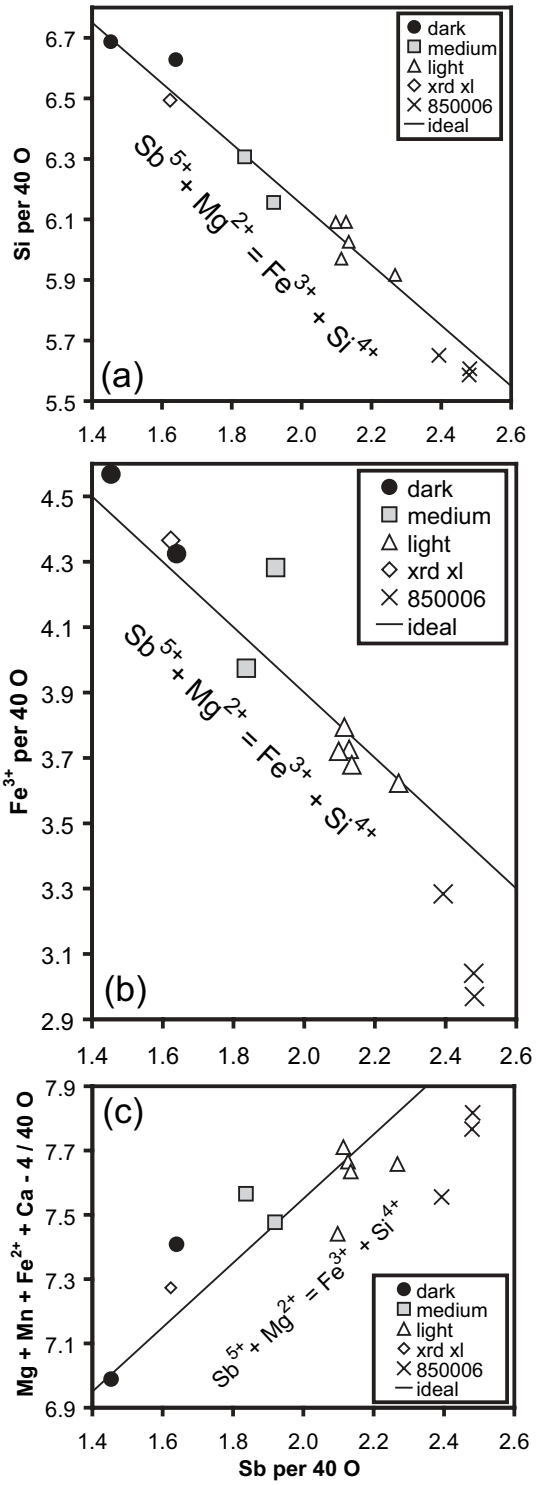

FIGURE 8. Composition of type 2 welshite (sample 900030 and of one crystal in sample 850006). Ideal refers to the substitution summing to $Sb^{5+} + Mg^{2+} = Fe^{3+} + Si^{4+}$. Dark, medium, and light refer to relative brightness in back-scattered electron images in sample 900030 (Fig. 4); xrd xl = average of analyses at 8 spots on the crystal used for attempted crystal structure refinement. The total octahedral occupancy is corrected for Mn substitution of Ca by adding Ca – 4 to the ordinate in **c**.

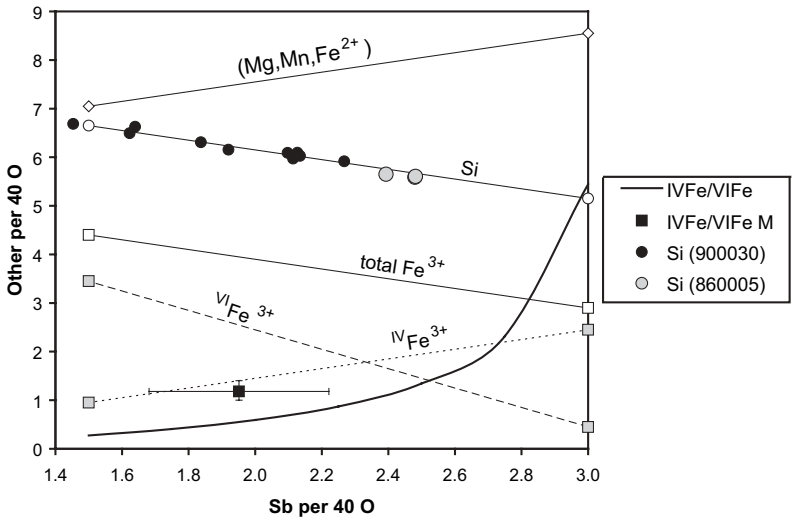

FIGURE 9. Ideal variations in Si and Fe^{3+} with Sb between two end-members $Ca_4(Mg,Mn,Fe)_{8.55}Fe_{0.45}Sb_{3.0}Si_{5.15}As_{0.45}Be_{3.45}Al_{0.5}Fe_{2.45}O_{40}$ and $Ca_4(Mg,Mn,Fe)_{7.05}Fe_{3.45}Sb_{1.5}Si_{6.65}As_{0.45}Be_{3.45}Al_{0.5}Fe_{0.95}O_{40}$. M refers to the $^{IV}Fe^{3+}/^{VI}Fe^{3+} = 0.52/0.44$ determined by Mössbauer spectroscopy and the error bars estimated from the ±0.04 uncertainty (Table 6). The plotted Sb content and error bars are, respectively, the average and standard deviation of the nine analyses on the crystal illustrate in Figure 4. The Si contents (measured) are taken from Figure 8.

The measured compositions of welshite in sample 900030 and the Sb-poor crystal of 850006 can be rationalized as a solid solution between two idealized end-members $Ca_4(Mg,Mn,Fe)_{8.55}Fe_{0.45}Sb_{3.0}Si_{5.15}As_{0.45}Be_{3.45}Al_{0.5}Fe_{2.45}O_{40}$ and $Ca_4(Mg,Mn,Fe)_{7.05}Fe_{3.45}Sb_{1.5}Si_{6.65}As_{0.45}Be_{3.45}Al_{0.5}Fe_{0.95}O_{40}$ with Fe as Fe^{3+} except as a substituent for Mg and Mn (total cationic charge 80.05) (Fig. 9). The former differs from the end-member $Ca_4Mg_9Sb_3Si_6Be_3AlFe_2O_{40}$ proposed for type 1 compositions through a substitution approximated by $^{IV}Be + {}^{VI}Fe = {}^{IV}Si + {}^{VI}Mg$ (Fig. 5) with charge balance provided by adjustments in the contents of most all constituents. Except for Sb > 2.6, compositional variations are tightly constrained for type 2, so we have not attempted to simplify the corresponding end-member compositions any further (Table 8).

We have not proposed a hypothetical Sb-free welshite, $Ca_4(Mg_6Fe_6)(Si_9Be_3)O_{40}$ end-member, which could be obtained by adding three equivalent net exchanges $^{M}Fe^{3+} + {}^{VI}Fe^{3+} + {}^{IV}Si^{4+} = {}^{M}Sb^{5+} + {}^{VI}Mg^{2+} + {}^{IV}Fe^{3+}$ to $Ca_4Mg_9Sb_3Si_6Be_3AlFe_2O_{40}$ (and including $^{IV}Fe^{3+}$ for $^{IV}Al^{3+}$). The partial structure refinement of welshite NRM900030 has shown that the Sb content is reduced on all three M7, M3A, and M4A sites simultaneously, so that there is no obvious constraint for the presence of Sb in one site over the others. It is clear, however, that the Sb^{5+} cations play a role in the welshite structure by satisfying the electrostatic bond strength sums around several of the O atoms. For instance, the O8A atom is bonded to M7, M1, T2A, and M9 (Fig. 1) with a bond strength sum of 5/6 + 2/6 + 2/4 + 2/7 = 1.95, close to the expected value of 2. In an Sb-free welshite with a random Mg^{2+}/Fe^{3+} mixing on the M sites, the bond strength sum for O8A would be reduced to 2.5/6 + 2.5/6 + 2/4 + 2/7 = 1.62. Similarly, the bond strength sum around O12 bonded to M4A, M5, M5A, and T4 would be reduced to 2.5/6 + 2.5/6 + 2.5/6 + 2/4 = 1.75. Therefore, we suggest that the existence of an Sb-free welshite is unlikely due to the significant underbonding that would result for several O atoms involved in the (Mg^{2+}/Fe^{3+})-O-Be^{2+} linkages replacing the Sb^{5+}-O-Be^{2+} linkages. The composition of welshite NRM900030 with the lowest Sb content of ~1.5 Sb per 40 O (Table 7) corresponds to average occupancies of 50% Sb + 50% Fe^{3+} on each of the M7, M3A, M4A sites. This cation distribution would yield bond strength sums around the bridging O atoms that are slightly reduced but within acceptable range of the expected values. As a result, this composition could be proposed as the low-Sb end-member of the welshite solid solution associated with the exchange $(^{M}Fe^{3+} + {}^{VI}Fe^{3+} + {}^{IV}Si^{4+})(^{M}Sb^{5+} + {}^{VI}Mg^{2+} + {}^{IV}Fe^{3+})_{-1}$.

WHAT IS WELSHITE?

Moore (1978) introduced welshite with a relatively simple composition $Ca_4Mg_8Fe^{3+}_2Sb_2O_4[Si_8Be_4O_{36}]$ (Table 8), one now generally given for this mineral in authoritative references (e.g., Strunz and Nickel 2001). Analyses of welshite deviate markedly from this formula, and we recommend that its use be discontinued. Hawthorne and Huminicki (2002) proposed four end-members, none of which correspond to a known welshite composition although a 50-50 mixture of the second and third listed in Table 8 correspond to one of our end-members. Most welshite crystals are a mixture of an Al and an Fe end-member related by a homovalent Al = Fe substitution on tetrahedral sites (type 1; Table 8), whereas a few crystals have more complex compositions (type 2; Table 8). One crystal is intermediate in composition between the two types (Fig. 5). Although no one end-member can be considered truly representative of welshite overall, $Ca_4Mg_9Sb_3O_4[Si_6Be_3AlFe_2O_{36}]$ comes the closest to most analyzed compositions (Fig. 7), and we recommend this formula for citation in databases. Our preferred generalized formula for welshite that encompasses close to all variations revealed to date is $(Ca,Mn)_4(Mg,Mn,Fe^{2+},Fe^{3+})_9(Sb,Fe^{3+})_3O_4[(Si,As)_6(Be,Al)_4(Al,Fe^{3+})_2O_{36}]$.

Given the wide variation in welshite composition, there could be more than one species present. There does not appear to be a distinct species based on Sb because Sb appears to be dominant in at least one of the sites it occupies (M7, M3A, and M4A), but

two potential species include one in which Fe is dominant at T5 and T6A and another in which Al is dominant at these sites. Our structure crystal is intermediate (Table 4b).

Our results show that octahedral cations having high valence are required for stabilizing the welshite structure by providing the necessary charge compensation for its elevated content of tetrahedral Be^{2+}. No attempts have yet been made to synthesize a welshite phase, as has been done previously for surinamite (de Roever et al. 1981; Hölscher et al. 1986) and beryllian sapphirine (Christy et al. 2002). But we predict that a successful synthesis of welshite or compounds related to welshite will require the presence of either Sb^{5+} cations or possibly other highly charged six-coordinated cations of similar size, such as Nb^{5+} or Ti^{4+}.

The simultaneous presence of high Sb and high Be contents in welshite appears to be one of its defining characteristics. It is directly associated with the charge ordering observed in the crystal structure and with the resulting *P*1 symmetry. These two constituents make welshite unique among the minerals of the aenigmatite-sapphirine-surinamite group.

ACKNOWLEDGMENTS

We thank J. Smyth (University of Colorado) for providing the software originally written by Y. Ohashi and used for the calculation of electrostatic potentials, and Paul Burger for obtaining and processing the SIMS Li data. We thank an anonymous reviewer and Richard Thompson for their comments on an earlier draft and Sergey Krivovichev for his editorial handling. E.S.G.'s research was supported by U.S. National Science Foundation grants OPP-00887235. UH acknowledges support from research grants from the Swedish Research Council (VR).

REFERENCES CITED

Barbier, J., Grew, E.S., Moore, P.B., and Su, S.-C. (1999) Khmaralite, a new beryllium-bearing mineral related to sapphirine: A superstructure resulting from partial ordering of Be, Al, and Si on tetrahedral sites. American Mineralogist, 84, 1650–1660.

Barbier, J., Grew, E.S., Hålenius, E., Hålenius, U., and Yates, M.G. (2002) The role of Fe and cation order in the crystal chemistry of surinamite, $(Mg,Fe^{2+})_3(Al,Fe^{3+})_3O[AlBeSi_3O_{15}]$: A crystal structure, Mössbauer spectroscopic, and optical spectroscopic study. American Mineralogist, 87, 501–513.

Bonaccorsi, E., Merlino, S., and Pasero, M. (1989) The crystal structure of the meteoritic mineral krinovite, $NaMg_2CrSi_3O_{10}$. Zeitschrift für Kristallographie, 187, 133–138.

——— (1990) Rhönite: structural and microstructural features, crystal chemistry, and polysomatic relationships. European Journal of Mineralogy, 2, 203–218.

Bruker (2000) SAINT program, version 6.02a. Bruker AXS Inc., Madison, Wisconsin.

Cannillo, E., Mazzi, F., Fang, J.H., Robinson, P.D., and Ohya, Y. (1971) The crystal structure of aenigmatite. American Mineralogist, 36, 427–446.

Christy, A.G., Tabira, Y., Hölscher, A., Grew, E.S., and Schreyer, W. (2002) Synthesis of beryllian sapphirine in the system MgO-BeO-Al_2O_3-SiO_2-H_2O and comparison with naturally occurring beryllian sapphirine and khmaralite. Part 1: Experiments, TEM, and XRD. American Mineralogist, 87, 1104–1112.

Coey, J.M.D.(1984) Mössbauer spectroscopy of silicate minerals. In G.J. Long, Ed., Mössbauer Spectroscopy Applied to Inorganic Chemistry, p. 443–509. Plenum Press, New York.

de Roever, E.W.F., Lattard, D., and Schreyer, W. (1981) Surinamite: a beryllium-bearing mineral. Contributions to Mineralogy and Petrology, 76, 472–473.

Dyar, M.D., Wiedenbeck, M., Robertson, D., Cross, L.R., Delaney, J.S., Ferguson, K., Francis, C.A., Grew, E.S., Guidotti, C.V., Hervig, R.L., Hughes, J.M., Husler, J., Leeman, W., McGuire, A.V., Rhede, D., Rothe, H., Paul, R.L., Richards, I., and Yates, M. (2001) Reference minerals for the microanalysis of light elements. Geostandards Newsletter, 25, 441–463.

Engström, N. (1874): Analyses of two lithium-bearing minerals from Långbanshyttan. Geologiska Föreningens i Stockholm Förhandlingar, 2, 468–470 (in Swedish).

Evensen, J.M. and London, D. (2002) Experimental silicate mineral/melt partition coefficients for beryllium and the crustal Be cycle from migmatite to pegmatite. Geochimica et Cosmochimica Acta, 66, 2239–2265.

——— (2003) Experimental partitioning of Be, Cs, and other trace elements between cordierite and felsic melt, and the chemical signature of S-type granite. Contributions to Mineralogy and Petrology, 144, 739–757.

Grew, E.S., Hålenius, U., Kritikos, M., and Shearer, C.K. (2001) New data on welshite, e.g., $Ca_2Mg_{3.8}Mn^{2+}_{0.6}Fe^{2+}_{0.1}Sb^{5+}_{1.5}O_2[Si_{2.8}Be_{1.7}Fe^{3+}_{0.65}Al_{0.7}As_{0.17}O_{18}]$, an aenigmatite-group mineral. Mineralogical Magazine, 65, 665–674.

Grew, E.S., Barbier, J., Britten, J., Yates, M.G., Polyakov, V.O., Shcherbakova, E.P., Hålenius, U., and Shearer, C.K. (2005) Makarochkinite, $Ca_2Fe^{2+}_4Fe^{3+}TiSi_4BeAlO_{20}$, a new beryllosilicate member of the aenigmatite-sapphirine-surinamite group from the Il'men Mountains (southern Urals), Russia. American Mineralogist, 90, 1402–1412.

Grew, E.S., Yates, M.G., Shearer, C.K., Hagerty, J.J., Sheraton, J.W., and Sandiford, M. (2006) Beryllium and other trace elements in paragneisses and anatectic veins of the ultrahigh-temperature Napier Complex, Enderby Land, East Antarctica: The role of sapphirine. Journal of Petrology, 47, 859–882.

Hawthorne, F.C. and Huminicki, D.M.C. (2002) The crystal chemistry of beryllium. In E.S. Grew, Ed., Beryllium: Mineralogy, Petrology, and Geochemistry, 50, p. 333–403. Reviews in Mineralogy and Geochemistry, Mineralogical Society of America, Chantilly, Virginia.

Hölscher, A., Schreyer, W., and Lattard, D. (1986) High-pressure, high-temperature stability of surinamite in the system MgO-BeO-Al_2O_3-SiO_2-H_2O. Contributions to Mineralogy and Petrology, 92, 113–127.

Jernberg, P. and Sundqvist, B. (1983) A versatile Mössbauer analysis program. Uppsala University, Institute of Physics (UUIP-1090).

Kunzmann, T. (1999) The aenigmatite-rhönite mineral group. European Journal of Mineralogy, 11, 743–756.

Merlino, S. (1972) X-ray crystallography of krinovite. Zeitschrift für Kristallographie, 136, 81–88.

Moore, P.B. (1967) Eleven new minerals from Långban, Sweden. Canadian Mineralogist, 9, 301 (abstract).

——— (1971) Mineralogy & chemistry of Långban-type deposits in Bergslagen, Sweden. Mineralogical Record, 1(4), 154–172.

——— (1978) Welshite, $Ca_2Mg_4Fe^{3+}Sb^{5+}O_2[Si_4Be_2O_{18}]$, a new member of the aenigmatite group. Mineralogical Magazine, 42, 129–132.

Moore, P.B. and Araki, T. (1983) Surinamite, ca. $Mg_3Al_4Si_3BeO_{16}$: its crystal structure and relation to sapphirine, ca. $Mg_{2.8}Al_{7.2}Si_{1.2}O_{16}$. American Mineralogist, 68, 804–810.

Nysten, P., Holtstam, D., and Jonsson, E. (1999) The Långban minerals. In D. Holtstam and J. Langhof, Eds., Långban. The Mines, Their Minerals, Geology, and Explorers, p. 89–183. Swedish Museum of Natural History, Raster Förlag, Stockholm.

Pouchou, J.L. and Pichoir, F. (1984) A new model for quantitative X-ray microanalysis. I. Application to the analysis of homogeneous samples. La Recherche Aérospatiale, 3, 13–36.

Shannon, R.D. (1976) Revised effective ionic radii and systematic studies of interatomic distances in halides and chalcogenides. Acta Crystallographica, A32, 751–767

Sheldrick, G.M. (1996) SADABS, Siemens area detector absorption correction software. University of Göttingen, Germany.

——— (1997) SHELXL97, program for the refinement of crystal structures. University of Göttingen, Germany.

Smyth, J.R. (1989) Electrostatic characterization of oxygen sites in minerals. Geochimica et Cosmochimica Acta, 53, 1101–1110.

Strunz, H. and Nickel, E.H. (2001) Strunz Mineralogical Tables. Chemical-Structural Mineral Classification System (9th edition), 870 p. Schweizerbart'sche Verlagsbuchhandlung, Stuttgart.

MANUSCRIPT RECEIVED FEBRUARY 28, 2006
MANUSCRIPT ACCEPTED JUNE 29, 2006
MANUSCRIPT HANDLED BY SERGEY KRIVOVICHEV